Electron scattering from Xe: the relation between the differential elastic cross section and shape and intensity of the energy loss spectra

2010 J. Phys. B: At. Mol. Opt. Phys. 43 215201

(http://iopscience.iop.org/0953-4075/43/21/215201)

IOP Publishing | Journal of Physics B: Atomic, Molecular and Optical Physics
J. Phys. B: At. Mol. Opt. Phys. **43** (2010) 215201 (7pp) | doi:10.1088/0953-4075/43/21/215201

Electron scattering from Xe: the relation between the differential elastic cross section and shape and intensity of the energy loss spectra

Maarten Vos

Atomic and Molecular Physics Laboratories, Research School of Physics and Engineering, Australian National University, Canberra, ACT, Australia

E-mail: maarten.vos@anu.edu.au

Received 14 July 2010, in final form 27 August 2010
Published 12 October 2010
Online at stacks.iop.org/JPhysB/43/215201

Abstract
The measurement of the energy loss spectra of energetic electrons scattered from Xe over large angles is reported. The incoming energy was chosen between 600 eV and 1550 eV. The calculated Xe elastic scattering cross section has a sharp minimum for 750 eV electrons near 135°. This minimum is confirmed by studying a Xe–H_2 mixture and separating their elastic peak based on the recoil effect. The energy loss part of the Xe spectra is rich in structure. Surprisingly the shape and intensity (relative to the elastic peak) changes dramatically if one approaches the scattering conditions for which the elastic cross section has a minimum. These observations are rationalized by describing the inelastic intensity semi-classically, as a consequence of a two-step process occurring at the same atom involving scattering from the nucleus and an electronic excitation. The change in shape of the loss spectra is attributed to a large increase in relative intensity of the dipole-forbidden transitions near sharp minima in the elastic cross section.

(Some figures in this article are in colour only in the electronic version)

1. Introduction

Electron scattering from atoms is usually divided into elastic scattering and inelastic scattering. In the former the electron exchanges momentum $\boldsymbol{q}$ with the atom, and is deflected with no or very small energy loss. In the latter the scattered electron changes the electron configuration of the scattering atom, without transferring momentum to the nucleus. This simple picture may describe adequately the intensity observed at small momentum transfer, but predicts that the inelastic energy loss features should be virtually absent at large momentum transfer, as there is only a finite amount of momentum that can be absorbed by an electronic excitation of the target. In reality the intensity of the inelastic features remains finite, and, for large values of the scattering angle θ, and incoming energies E_0 in the keV range, the ratio of the elastic and inelastic scattering intensity is generally only a weak function of θ [1].

The assumption that the inelastic intensity at high momentum transfer is purely a consequence of an electronic excitation is thus wrong. Such a process is more complicated, involving momentum transfer to the nucleus as well. In simple terms the intensity is a consequence of elastic and inelastic scattering of the projectile by the *same* atom and hence it cannot be described by a first-Born-type approach. For the case of e^- scattering from H and He, this was discussed by Geltman and Hidalgo as early as 1972 [2, 3], and Bonham used a second Born approach to describe such conditions for electrons scattered from Hg [4]. The situation was recently reviewed by Kelsey from a theoretical point of view [5].

For N_2 this picture was used recently to explain the large deviation at large q values in spectra obtained by non-resonant inelastic x-ray scattering (NRIXS) measurements (where the first Born approximation applies) and electron energy loss spectroscopy (EELS) (where the first Born approximation fails) [6]. The interaction of the probing electron with the nucleus can be described by presenting its wavefunction not by a plane wave but by a distorted wave. Such distorted-wave calculations have been done for Xe only at much lower energies (30 eV) [7].

The differential elastic cross section of heavy atoms shows very profound structures at intermediate energies and large scattering angles. For example, the differential elastic cross section of Xe is predicted to have a sharp dip near 90° at 400 eV (see [8] and references therein) and this minimum was observed experimentally by Williams and Crowe [9]. Another sharp minimum is predicted near 135° at 750 eV. Here the Xe differential elastic cross section is calculated to drop by two orders of magnitude. This sharp minimum was recently confirmed by measuring the intensity ratio of elastic scattering from a gas mixture of H_2 and Xe, where the Xe and H elastic peaks were separated due to the recoil effect [10].

Near the minimum of the cross section at 135° and $E_0 = 750$ eV the momentum transfer is 13.7 au (atomic units), considerably more than what can be accommodated by an electronic excitation. Surprisingly, as we will see, the measured energy loss intensity is easily measurable. We assume that momentum transfer due to interaction with the nucleus has to be considered as part of the process that leads to energy loss intensity at large momentum transfer.

If, as sketched here, the process leading to inelastic excitations at large momentum transfer involves scattering from the nucleus, then it becomes of interest to investigate the intensity and shape of the energy loss spectra near a sharp minimum in the differential elastic scattering cross section. This is the subject of this paper. We will demonstrate that the intensity (relative to the elastic peak) and shape of the energy loss spectra vary greatly under these conditions. The shape variations are consistent with a large increase in the contribution of dipole-forbidden transitions, when the elastic differential cross section has a sharp minimum.

In a previous paper we investigated this system at higher energies, and at lower energy resolution [1], and discussed the implications of the observed energy loss structures for modelling the transport of electrons in matter. The current work indicates that shortcomings in the traditional approach of electron transport in matter (describing the transport as a consequence of uncorrelated elastic and inelastic scattering events) should show up most clearly when deep minima in the differential elastic scattering cross section are probed by the experiment.

2. Experimental details

The experimental spectrometer is described in some detail in [11]. The spectrometer was designed to study the recoil effect (see e.g. [12]), but has been used more recently to study the energy loss spectrum after large momentum transfer collisions. Briefly it consists of an unmonochromatized electron gun with a BaO cathode, a set of slit lenses followed by a hemispherical analyser with a two-dimensional readout allowing for simultaneous measurement of a range of energies and outgoing directions. The Xe gas is introduced using a needle (diameter 0.7 mm). The aperture limiting the electron flux entering the slit lens system is placed 145 mm from the interaction region and is 0.5 mm wide and 40 mm long, but only the central 20 mm are used in the actual measurement by limiting the acquired data to only part of the two-dimensional detector. The range of θ angles measured is determined by the 0.5 mm width of the entrance slit in combination with the ≈0.7 mm diameter of the interaction region and thus $\Delta\theta \approx 0.5°$. The spectrometer can run up to electron energies of 8 keV, and the pressure was $\approx 3\times10^{-6}$ Torr. Changing the pressure by a factor of 4 results only in minor (10% or so) changes in the ratio of the elastic and inelastic intensities. This shows that in a large majority of the cases the inelastic intensity is not due to electrons scattering elastically from one atom, and inelastically from another atom. In that case the inelastic to elastic signal ratio would increase linearly with Xe pressure.

The analyser is fixed, and the gun can be mounted on either one of three flanges such that the scattering angle is 45°, 90° and 135°. The original readout of the detector was based on a resistive anode. This has since been replaced by a phosphor screen–camera combination [13]. Together with several other small changes (reduced diameter of the gas needle, set of slits at the entrance of the hemispherical analyser) this has resulted in an improvement of the energy resolution of 0.6 eV (for a 300 nA beam) to 0.25–0.3 eV (for a 50 nA beam). A measurement takes typically between a few days and a week, depending on the cross section, width of the energy loss scan and beam current used.

3. Experimental results

The interpretation of the experiment is based on the presence of a sharp minimum in the differential *elastic* cross section. Hence we summarize first how this sharp minimum was verified experimentally in [10] using a gas mixture of H_2 and Xe.

In figure 1 we show the differential elastic cross section for electrons scattering from Xe and H atoms as calculated by the ELSEPA program [14]. The cross section from the hydrogen atom at a large angle follows closely the Rutherford cross section, but the cross section from Xe is predicted to have much more structure. In particular, at 750 eV there is a very strong (two orders of magnitude) dip near $\theta = 135°$. This dip becomes broader and less deep when E_0 is chosen away from 750 eV.

As our detector position is fixed at 135° , we will measure the elastic peak intensity at a constant scattering angle as a function of incoming energy E_0. By measuring a mixture of Xe and H_2 (and assuming that the H cross section is described well by the ELSEPA program), we can verify the existence of the deep minimum in the Xe cross section at 135°. This is because the elastic peaks of H and Xe appear at slightly different energies as explained next. The electron (momentum $\boldsymbol{k}_0$ before the collision, $\boldsymbol{k}_1$ after the collision) transfers momentum $\boldsymbol{K} = \boldsymbol{k}_1 - \boldsymbol{k}_0$ to the scattering atom and the kinetic energy of this atom (mass m_a) changes by $K^2/2m_a$. The electron energy is reduced by this amount. For this reason (the recoil effect) the elastic peaks of H and Xe are separated

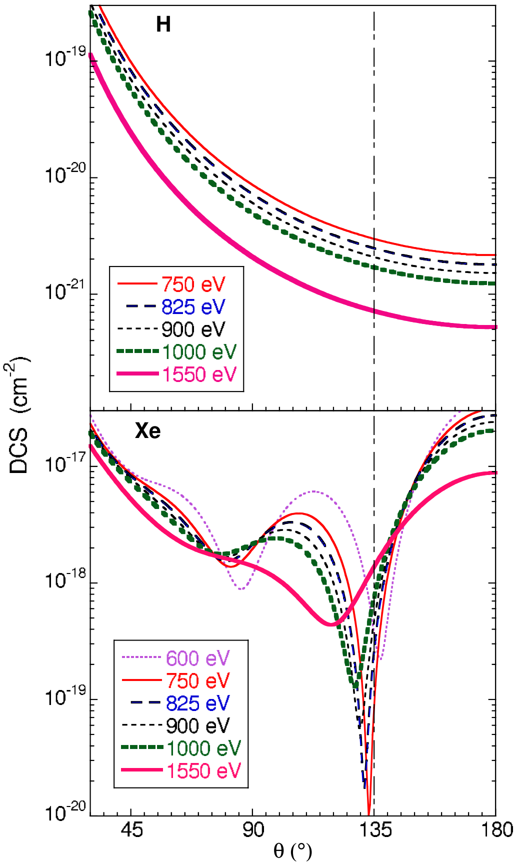

Figure 1. The differential elastic cross section of H (top) and Xe (bottom) as calculated using ELSEPA, for the energies indicated.

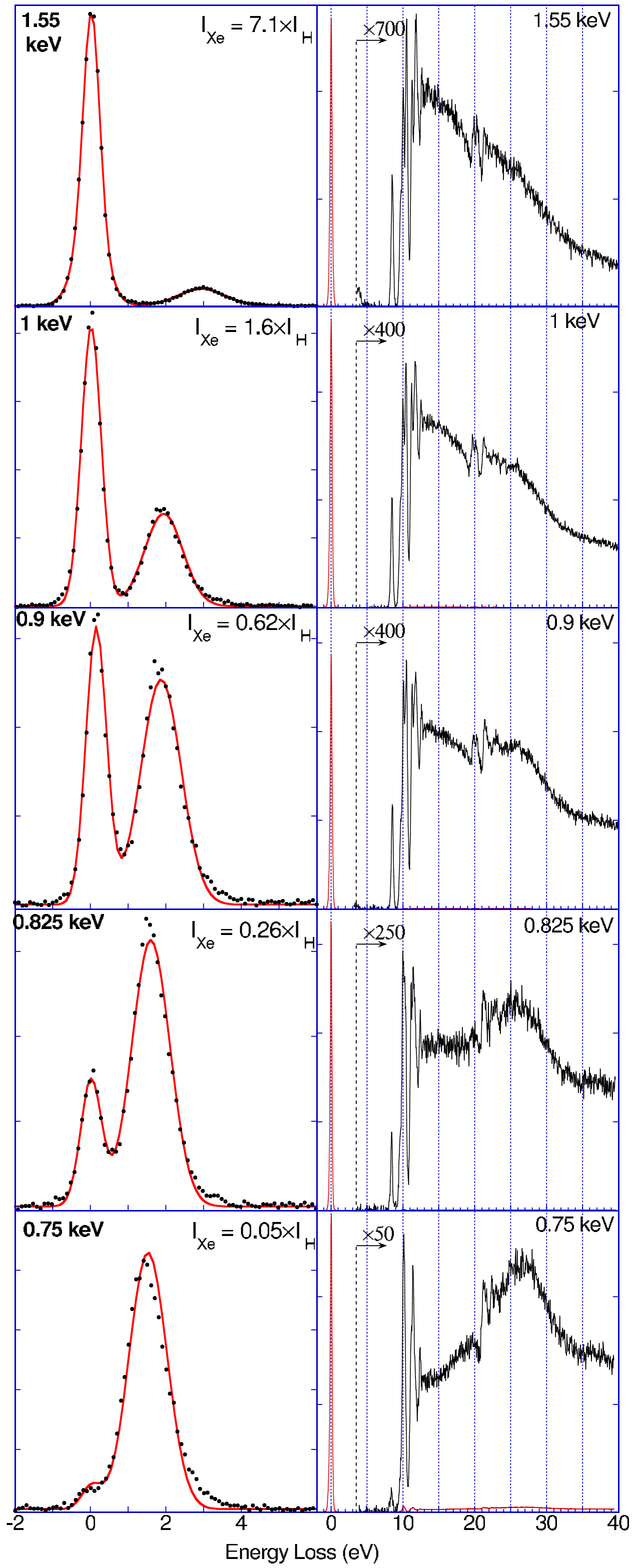

Figure 2. The elastic peaks of H and Xe as measured for a H_2–Xe gas mixture for E_0 values as indicated are shown in the left panels. The elastic peak is split due to the recoil effect as explained in the text. The peak near zero energy loss is due to Xe; the peak due to H is near 3 eV energy loss for the 1.55 keV measurement, decreasing to 1.5 eV energy loss for the 750 eV measurement. The right panels show the measurement for *pure* Xe at the same energy over a larger energy loss window. There is a large range in shape and relative intensity of the Xe loss spectrum.

in energy. For more details see [10, 15]. Indeed two peaks with a large variation in intensity are seen in the left column of figure 2. The intensity ratio of the H and Xe elastic peaks varies wildly but follows closely the expectations based on the ELSEPA program as was shown in [10].

We measured for the same values of E_0 and scattering angle also the energy loss spectra for electrons scattering from *pure* Xe. These spectra are shown in the right column of figure 2. At all energies there is an abundance of structure in the spectra. The intensity of the loss part, relative to the elastic peak, varied widely. The largest loss feature (near 10 eV energy loss) is 700× less intense than the elastic peak at 1.55 keV, but only 50× weaker than the elastic peak at 750 eV.

Besides the overall intensity, the shape of the spectra also changes dramatically with E_0 as one approaches the minimum in the cross section. This applies both to the discrete peaks as well as the continuum part of the loss spectra. These changes extend over a larger energy loss range. In figure 3 we show spectra taken at 750 eV and 1000 eV from 0 to 140 eV energy loss. Near 65 eV energy loss there are more weak discrete features associated with the excitation of the Xe 4d electrons followed by two broader, overlapping peaks with maxima near 80 eV and 110 eV . The latter structure dominates at 750 eV and is closer in energy loss to the resonance observed in electron momentum spectroscopy (EMS) [16], than to that seen in photo absorption or dipole (e, 2e) experiments (e.g. [17]). This energy region has also been studied in energy

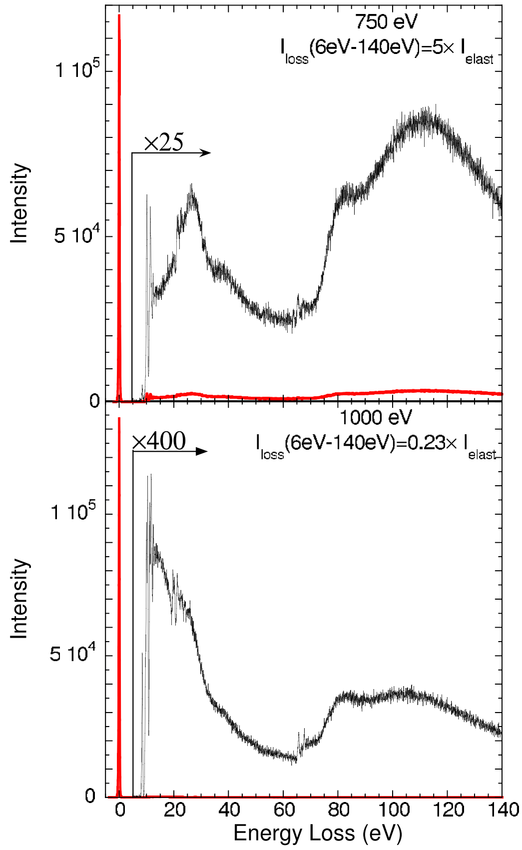

Figure 3. The energy loss spectra at 750 eV and 1000 eV over a larger range of energy losses. Note that in the 750 eV case the area of the loss features exceeds that of the elastic peak by a factor of 5, whereas at 1000 eV it is four times less.

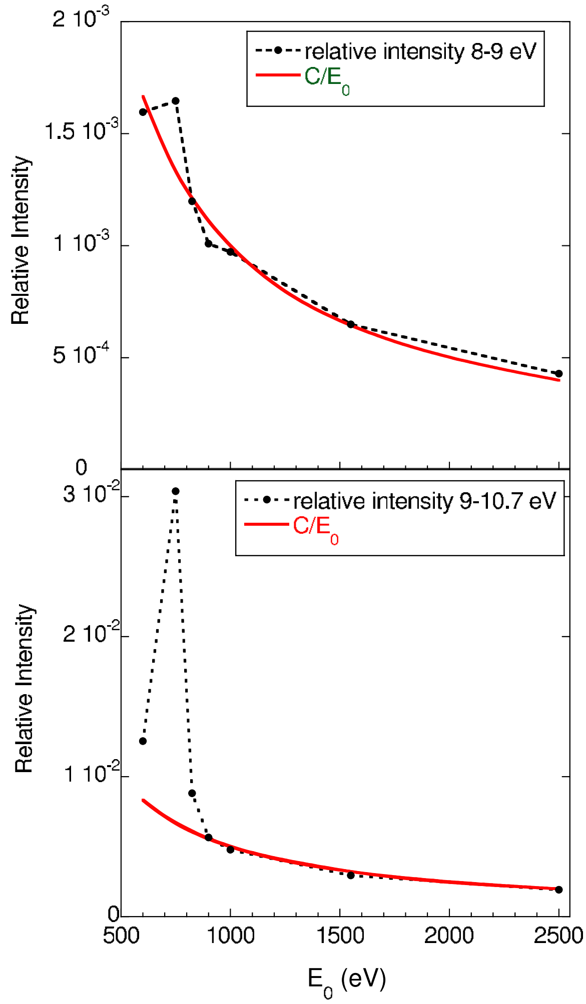

Figure 4. The intensity between 8 and 9 eV energy loss as a fraction of the elastic peak intensity (top) and the same for the intensity between 9 and 10.7 eV (bottom). The full line is proportional to $1/E_0$ and is given for comparison.

loss measurements at smaller scattering angles by Boechat-Roberty *et al* [18]. They observed, using an incoming beam with $E_0 = 1045$ eV, a maximum at energy losses of 95 eV for small angle deflections (1.5°) shifting to ≈105 eV for 17° deflections. More interestingly, in the context of this paper, the ratio of the elastic peak intensity to the energy loss intensity changes dramatically. At 1000 eV, the integrated intensity of the loss spectrum from its onset to 140 eV is 4× *less* than the intensity of the elastic peak. At 750 eV, the loss spectrum, integrated over the same energy range, is 5× *more* intense than the elastic peak.

This increase in relative intensity of the energy loss part of the spectrum can be seen as a consequence from the reduction in the intensity of the elastic peak, due to the dip in the cross section, not being mirrored in a similar decrease in the inelastic part of the spectrum. In our previous study [1] we found that at higher energies (>1 keV) the intensity of the loss part, relative to the elastic peak at a given angle, is proportional to $1/E_0$. Hidalgo and Geltman [3] postulated that for He the absolute intensity of the loss features should decrease as $1/E_0^3$ in agreement with our observation for Xe as, under these conditions, the He elastic differential cross section follows the Rutherford cross section closely (i.e. it is proportional to $1/E_0^2$).

In figure 4 we plot the intensity of the first peak corresponding to the 8.4 eV $6s[1\frac{1}{2}]_1^0$ excitation relative to that of the elastic peak and compare it to a C/E_0-type dependence. There is a slight increase at 750 eV above what is expected based on C/E_0 behaviour, and at the lowest energy measured (600 eV) the observed intensity is again on the C/E_0 line.

Unfortunately, with our current resolution the other structures observed are due to overlapping excited states. For all spectra there is a pronounced minimum near 10.7 eV. Hence we integrated the spectra from 9 to 10.7 eV and plotted this quantity as well as a function of C/E_0. Now we see a strong deviation from C/E_0-type behaviour at 750 eV. It is thus clear that the change in shape of the spectra seen in the right panel of figure 2 is not due to a decrease in the $6s[1\frac{1}{2}]_1^0$ state, but due to an increase in the intensity between 9 and 10.7 eV.

There exist many studies of Xe at much lower momentum transfer (and much better energy resolution) (e.g. [17, 19–21]) and some at comparable momentum transfer [22]. The discrete states contributing to the loss spectrum are thus well known and we can use this knowledge to analyse our spectra in some more detail.

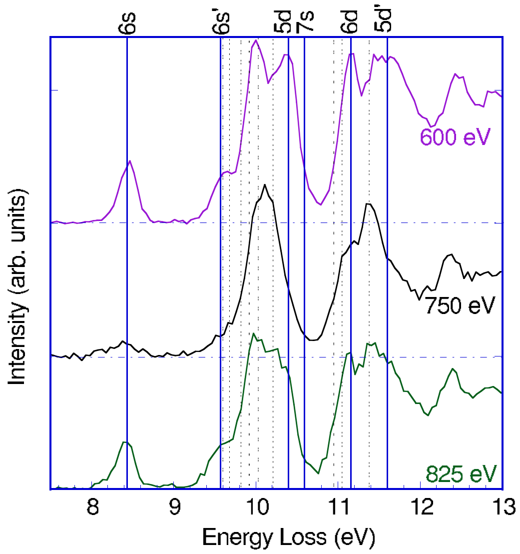

Figure 5. A comparison of the shape of the energy loss spectra at 600, 750 and 825 eV . The solid vertical lines correspond to dipole-allowed transitions, and the dotted lines to dipole-forbidden transitions. The shape of the 600 eV spectrum is much closer to the shape of the 825 eV spectrum than to the shape of 750 eV spectrum. The difference is consistent with a large enhancement of the non-dipole contribution in the 750 eV spectrum.

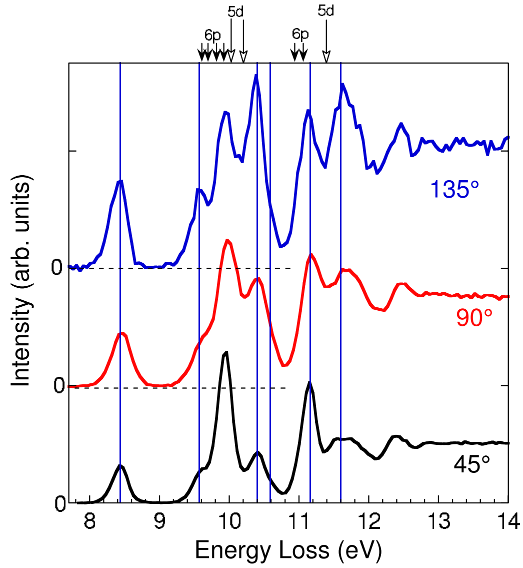

Figure 6. A comparison of the spectra taken at different angles for $E_0 = 1$ keV.

In figure 5 we zoom in on the low energy loss range (7–13 eV) for the 600, 750 and 825 eV measurements. The first few (well-known) dipole-allowed excitations ($\Delta l = 1$) are indicated by the solid vertical lines (the 6s$\left[1\frac{1}{2}\right]_1^0$ state at 8.44 eV, the 6s$'\left[0\frac{1}{2}\right]_1^0$ state at 9.56 eV, the 5d$\left[1\frac{1}{2}\right]_1^0$ state at 10.40 eV, the 7s$\left[1\frac{1}{2}\right]_1^0$ state at 10.59 eV, the 6d$\left[1\frac{1}{2}\right]_1^0$ state at 11.16 eV and the 5d$'\left[1\frac{1}{2}\right]_1^0$ state at 11.61 eV). Away from the minimum in the elastic cross section these positions line up with some of the significant maxima in the loss distribution. At the minimum in the elastic cross section all these peaks appear reduced in intensity, but, as we saw before, the interpretation that the non-dipole transitions are increased is more accurate.

Spectra taken at other angles have different shapes but the dipole-allowed transitions again line up with many of the maxima, as can be seen in figure 6 for 1 keV spectra taken at 45°, 90°and 135°. Here we also indicate the major non-dipole transitions as identified in [22], which are also shown as dashed and dotted lines in figure 5. These are dipole-forbidden 6p and 5d transitions.

In all spectra of figures 5 and 6 there is a strong peak near 10 eV. There are three states that contribute significantly to the intensity around 10 eV in [22], the 6p$\left[0\frac{1}{2}\right]_1$ state at 9.92 eV (actually the most intense of all peaks in the 90° spectrum of [22]), the 5d$\left[3\frac{1}{2}\right]_1^0$ state at 10.03 eV and the 5d$\left[2\frac{1}{2}\right]_1^0$ state at 10.21 eV. At the minimum of the elastic cross section this peak becomes even more pronounced and its position shifts somewhat to larger energy loss, indicating an increase in the relative intensity of the 5d contributions compared to the 6p contributions.

Thus we can be a bit more specific on the cause of the spike intensity at 750 eV in the 9–10.7 eV energy loss range. Near 750 eV the shape of the energy loss distribution indicates that the contribution of the dipole-allowed states is relatively minor. Thus the huge spike observed in the lower panel of figure 4 at 750 eV is due to an increase in intensity of the 5d states and to a lesser extent the 6p states. In the next section we present a simple semi-classical model explaining these observations

4. Simple model

In order to get some understanding of these observations we propose a simple model. We assume that the experimental result can be described as a consequence of two collisions. One collision is an elastic collision, with a differential cross section as calculated by e.g. ELSEPA, a cross section that could be measured by determining the elastic peak intensity as a function of angle. The other collision is an inelastic collision as can be measured in a small-angle scattering experiment. Such collisions have been studied in the literature extensively, and the results are usually presented in the form of generalized oscillator strength (GOS). In these experiments one determines the cross section for inelastic excitations as a function of (small) deflection angles and calculates the GOS as a function of the momentum transfer K, which is related to the inelastic differential cross section as

$$F(K) = \frac{W}{2}\frac{k_0}{k_1}K^2\left(\frac{d\sigma}{d\Omega}\right) \tag{1}$$

with W the excitation energy. These experiments are done for small momentum transfers that are (assumed to be) absorbed by the electronic excitation. Such an experiment is usually interpreted within the first Born approximation. For Xe, extensive GOS measurements have been published by Suzuki *et al* [23–25].

In our (qualitative) model we assume that the total deflection of the electron is due to an elastic scattering event over an angle θ and a much smaller deflection θ' due to the inelastic excitation. The 'sum' of θ and θ' should correspond to our detector angle of 135°. Of course there appears to be no reason for θ and θ' to be in the same plane. Thus for events with e.g. $\theta' = 2°$ it is possible that they are detected for $133 \leqslant \theta \leqslant 137°$.

From scattering experiments at small angles we know that the cross section for dipole-allowed transitions has a maximum at 0° and decreases rapidly with increasing scattering angle. From [23, 24] we know that the differential cross section for $E_0 = 500$ eV drops by one order of magnitude if the scattering angle is increased by 2.5° corresponding to a momentum transfer of 0.26 au. As the cross section under these conditions is well represented by the first Born approximation, it is dependent on the magnitude of K only; hence, at 750 eV we would expect the cross section to drop by an order of magnitude of 2° as, for a given scattering angle, K is proportional to $\sqrt{E_0}$. Thus a dipole-allowed transition does not change the direction of the impinging electron much. For detection an elastic deflection near 135° is still required. Hence the intensity of these features is almost as much reduced by the sharp minimum of the elastic cross section as the elastic peak itself.

The situation is somewhat different for the $6p\left[2\frac{1}{2}\right]_2$ and $6p\left[1\frac{1}{2}\right]_2$ transitions. Here the GOS increases for small K values almost proportional to K^2 [25] which means (see equation (1)) that the differential cross section drops relatively slowly for small angles. From the GOS measurements it is deduced that the DCS is reduced by a factor of 4 for $k = 0.4$ au, which corresponds to 3° at 750 eV.

For the $5d\left[3\frac{1}{2}\right]_3$ and $5d\left[2\frac{1}{2}\right]_3$ states the situation is more dramatically different. Here the DCS has a maximum at 5° for $E_0 = 500$ eV [24], corresponding to $K = 0.52$ au and is reduced from this maximum by a factor of 4 near 10°, corresponding to a momentum transfer over 1.0 au. At 750 eV, such a momentum transfer would correspond to a deflection of 8°. From figure 1 it is clear that such a deflection can shift us right out of the minimum of the elastic cross section, and the elastic DCS for the required elastic scattering event can increase by up to a factor of 10.

Thus especially for the 5d-type transitions the deflection due to this inelastic excitation can be enough to shift the required elastic scattering angle out of the deep minimum in the elastic DCS. Hence the intensity of these energy loss states is not as effectively reduced by the minimum in the elastic DCS. Hence the intensity of these states increases relative to the elastic peak. This is in perfect agreement with the observation in figure 4.

5. Conclusion and discussion

We have demonstrated that sharp features in the elastic scattering cross section have a dramatic influence on the shape of the loss features seen in large momentum transfer collisions. These changes can be understood, at least semi-quantitatively, using a semi-classical two-collision model. A two-step model is in line with the failure of the first Born approximation to explain the observed intensity under these conditions.

Near the minima in the elastic scattering cross section, the intensity or the energy loss part is extremely high. It is comparable to the intensity of the energy loss spectrum in condensed matter reflection energy loss spectroscopy (REELS) (see e.g. [26]). Such experiments are interpreted assuming no correlation between the elastic and inelastic scattering events. However, the results here show that under specific conditions, energy loss is very likely to occur at the atom that scatters the electron elastically. These experiments show thus that near sharp minima in the elastic cross section the correlation between elastic and inelastic events is the most pronounced. It is interested to note that under these conditions there are serious problems extracting the dielectric function from REELS spectra [27]. The processes described in this paper could be the underlying cause of this problem.

Acknowledgments

The author wants to thank Bob McEachran and Erich Weigold for stimulating discussions and critical reading of the manuscript. The research was made possible by funding from the Australian Research Council.

References

[1] Went M and Vos M 2009 *J. Electron Spectrosc. Relat. Phenom.* **169** 35
[2] Geltman S and Hidalgo M B 1971 *J. Phys. B: At. Mol. Phys.* **4** 1299
[3] Hidalgo M B and Geltman S 1972 *J. Phys. B: At. Mol. Phys.* **5** 617
[4] Bonham R A 1974 *J. Electron Spectrosc. Relat. Phenom.* **3** 85
[5] Kelsey E 2007 *Ann. Phys.* **322** 1925
[6] Bradley J, Seidler G, Cooper G, Vos M, Hitchcock A, Sorini A P, Schlimmer C and Nagle K 2010 *Phys. Rev. Lett.* **105** 053202
[7] Zuo T, McEachran R P and Stauffer A D 1991 *J. Phys. B: At. Mol. Opt. Phys.* **24** 2853
[8] Salvat F 2003 *Phys. Rev.* A **68** 012708
[9] Williams J F and Crowe A 1975 *J. Phys. B: At. Mol. Phys.* **8** 2233
[10] Vos M and Went M 2009 *J. Phys. B: At. Mol. Opt. Phys.* **42** 065204
[11] Vos M, Went M, Cooper G and Chatzidimitriou-Dreismann C 2008 *J. Phys. B: At. Mol. Opt. Phys.* **41** 135204
[12] Vos M 2010 *J. Chem. Phys.* **132** 074306
[13] Vos M, Went M and Weigold E 2009 *Rev. Sci. Instrum.* **80** 063302
[14] Salvat F, Jablonski A and Powell C J 2005 *Comput. Phys. Commun.* **165** 157
[15] Vos M 2002 *Phys. Rev.* A **65** 12703
[16] Takahashi M, Miyake Y, Watanabe N, Udagawa Y, Sakai Y and Mukoyama T 2007 *Phys. Rev. Lett.* **98** 013201
[17] Chan W F, Cooper G, Guo X, Burton G R and Brion C E 1992 *Phys. Rev.* A **46** 149
[18] Boechat-Roberty H M, Freitas J D, Almeida D P and de Souza G G B 2002 *J. Phys. B: At. Mol. Opt. Phys.* **35** 1409
[19] Geiger J 1977 *Z. Phys. A* **282** 129
[20] Khakoo M A, Trajmar S, LeClair L R, Kanik I, Csanak G and Fontes C J 1996 *J. Phys. B: At. Mol. Opt. Phys.* **29** 3455

[21] Yuan Z-S, Sakai Y, Umeda N, Fujita Y, Takayanagi T, Yamada C, Nakamura N, Ohtani S, Zhu L-F and Xu K-Z 2006 *J. Phys. B: At. Mol. Opt. Phys.* **39** 5097

[22] Urpelainen S, Huttula M, Kovala P, Makinen A, Calo A, Aksela S and Aksela H 2007 *J. Electron Spectrosc. Relat. Phenom.* **156–158** 145

[23] Suzuki T Y, Sakai Y, Min B S, Takayanagi T, Wakiya K, Suzuki H, Inaba T and Takuma H 1991 *Phys. Rev.* A **43** 5867

[24] Suzuki T Y, Suzuki H, Currell F J, Ohtani S, Takayanagi T and Wakiya K 1996 *Phys. Rev.* A **53** 4138

[25] Suzuki T Y, Suzuki H, Ohtani S, Takayanagi T and Okada K 2007 *Phys. Rev.* A **75** 032705

[26] Werner W, Went M R and Vos M 2007 *Surf. Sci.* **601** L109

[27] Werner W, Glantschnig K and Ambrosch-Draxl C 2009 *J. Phys. Chem. Ref. Data* **38** 1013